Materials Research. 2014; 17(3): 535-541
DOI: http://dx.doi.org/10.1590/S1516-14392014005000063

Surface Contact Fatigue Failure of a Case Hardened Pinion Shaft

Luciana Sgarbi Rossino*[a,b], *Danilo Borges Villarino de Castro*[c], *Jeferson Aparecido Moreto*[d], *Cassius Olivio Figueiredo Terra Ruchert*[e], *Dirceu Spinelli*[e], *José Ricardo Tarpani*[e]

[a]*Sorocaba Technological College – FATEC, Av. Engenheiro Carlos Reinaldo Mendes, 2015, Alto da Boa Vista, CEP 18013-280, Sorocaba, SP, Brazil*
[b]*Federal University of São Carlos – UFSCar, Rodovia João Leme dos Santos, Km 110, Bairro do Itinga, CEP 18052-780, Sorocaba, SP, Brazil*
[c]*Institute of Science and Technology – ICET, Universidade Paulista – UNIP, Av. Alberto Benassi, 200, Parque das Laranjeiras, CEP 14804-300, Araraquara, SP, Brazil*
[d]*Department of Chemistry, Federal Institute Goiano, Rodovia BR-153, Km 633, CEP 75650-000, Morrinhos, GO, Brazil*
[e]*Department of Materials Engineering – SMM, Engineering School of São Carlos – EESC, University of São Paulo – USP, Avenida Trabalhador Sancarlense, 400, Parque Arnold Schimidt, CEP 13566-590, São Carlos, SP, Brazil*

Received: January 24, 2012; Revised: April 8, 2014

An investigation was made to determine the causes of surface contact fatigue failure of a case hardened driver pinion located in the intermediate shaft of a reducer gearbox used in a sugar and alcohol mill. The examination of the component revealed the presence of a cemented layer substantially thicker than that generally specified for pinions devised for this application. This, associated with the massive presence of brittle threadlike carbon-rich cementite phase (Fe_3C) in prior austenite grain boundaries of the pinion teeth, favored surface crack nucleation and propagation during cyclic loading, leading to spallation of the contact surface with the counterpart gear, which impaired the system's operation. Poor carburization practice was discovered as the root cause of the mechanical failure, thus demanding the implementation of a new manufacturing route to avoid problems in similar load-bearing rotating components.

Keywords: *failure analysis, case hardened pinion, low-alloy steel, rotating component, surface contact fatigue*

1. Introduction

Gears are mechanical elements connected to rotating shafts whose contact surfaces must be carefully shaped to a specific profile to transmit uniform and continuous rotary motion. If the smaller wheel of the contacting pair, called the pinion shaft, is in the engine, the gear train will reduce the speed, thereby increasing the system's torque. On the other hand, if the main gear, which is the larger wheel of the contacting pair, is in the engine, the gear train will speed up the gearbox system and automatically decrease its torque. Shafts are used virtually in all machines that transmit rotational motion from one part to another, such as gears, pinions, roller bearings, and pulleys[1,2].

The main causes of in-service failure of case hardened gears are well established in the pertinent literature[3-11] and sometimes involve multiple and synergic mechanisms. For instance, Das et al.[3] observed that the rotating part of a diesel electric-power generator fractured by fatigue crack growth initiated at the fillet of the pinion teeth. These researchers concluded that a decrease in the contact area specified in the design of the failed teeth caused misalignment between the gear pinion and the ring gear, which subjected the system to severe wear in the region of highest stress contact, thus denoting a contact fatigue process. However, cyclic bending stresses above the material's fatigue limit, inadequate finishing of gear and pinion teeth and the presence of elongated sulfide inclusions in the microstructures of the two components contributed to progressive degradation of the mechanical system.

Strictly speaking, the above described surface contact fatigue process is defined as the evolution of damage that occurs when two specific moving surfaces touch each other repeatedly, allied to other processes such as corrosion, pit formation, wear debris and fatigue cracks. The damage process may reduce the component's load-bearing capacity or even result in complete failure of the components in contact with each other, make them functionless[7,8].

It is well known that exceptionally high cyclic contact pressure loads develop in real contacting rotating bodies (e.g., wheel-pinion pairs) and that the relative motion between them causes simultaneous rolling and sliding. This combined mechanical loading of the parts defines, to a great extent, the probability that surface contact fatigue will develop, which is why this phenomenon is commonly called rolling-sliding contact fatigue (RSCF). One or both of the bodies in contact also often undergoes fluctuating stresses resulting from vibrations or other forms of loading, which

*e-mail: jrpan@sc.usp.br

may lead to the propagation of cracks nucleated by surface contact fatigue, thus accelerating the fracture process of the materials involved[4].

RSCF was described by Basan et al.[9], whose information can be used for the prevention or subsequent identification and remedial actions against fatigue damage in power transmission gears. RSCF in gear/pinion tooth surfaces are generally due to the differences in tooth geometry, meshing conditions, material characteristics and type and parameters of surface carburization and hardening heat treatments.

The different types of damage attributed to RSCF of gear tooth flanks are: pitting (initial pitting, progressive pitting, micropitting and flake pitting), spalling and case crushing. The resulting damage is one of the most frequent causes of gear failure, and is directly related to the shear fatigue strength profiles of case hardened materials and the distribution of shear stresses caused by rolling-sliding contact loading[9]. Locations at which shear stresses exceed shear fatigue strength are the most likely sites for damage initiation. When a material is subjected to shear stress that is lower than its shear fatigue strength, no damage occurs. If it is subjected to shear stress exceeding its shear fatigue strength at the surface, the resulting damage is pitting. However, if the material is subjected to shear stress exceeding its shear fatigue strength immediately below surface, the resulting damage is flake pitting and/or spalling. Lastly, if the material is subjected to shear stress exceeding its shear fatigue strength in deep subsurface layers, it undergoes case crushing[10,11].

According to Basan et al.[9], one of the important features of gear/pinion tooth flanks surface treatments (case hardening) is the change in hardness from the surface to the core of the material. This behavior causes the material's fatigue strength to change in response to variations in surface hardness. Thus, the critical to fail position of gear/pinion tooth depends not only on the magnitude and distribution of stresses, but also on the distribution of hardness or fatigue strength, which is achieved by means of surface thermal and/or thermo-chemical treatments. An unfavorable stress-strain ratio, which is very often found in the transition area between a harder surface layer and a softer core, can result in localized plastic deformation of the material. Occasional overloading, which is inevitable during operation of the rotating machinery, can intensify this damage phenomenon, initiating subsurface cracks that can propagate below the surface, resulting in the separation and breaking off of large pieces of gear/pinion tooth flank material, and in some cases, even of large sections of the tooth. The main factors that contribute significantly to the development of this process are unsuitable depth of the hardened surface layer (either thinner or thicker than specified in the project stage), incorrect hardness profile in the hardened case and along the tooth height, insufficient core hardness (all of them resulting essentially from defective thermal and/or thermo-chemical treatments), occasional overloading during operation, errors in mesh due to manufacturing and assembly faults, and particularly the occurrence of cyclic stress that induces fatigue crack growth in the material. Thus, numerous factors can cause, acting individually or cooperatively, gear/pinion tooth to become damaged by rolling-sliding contact fatigue.

The challenge here is, therefore, to disclose the root cause(s) which led to the case hardened pinion failure during apparently normal in-service conditions of the studied gearbox.

2. Material and Components

The pinion analyzed in this study was manufactured with DIN 17CrNiMo6 steel (similar to SAE 8620[12]), cemented/carburized in a carbon rich atmosphere to reach the required 2.6 mm deep carbon rich surface layer, according to the DIN 50190 standard[13], and subsequently quenched (hardened) and tempered (Q&T) to obtain a structural piece exhibiting a hard and wear resistant surface layer allied to a very tough core to withstand repeated impact loads. According to the pinion design specification, macrohardness of the tooth flank must be 60-61 HRC, and 35-43 HRC at its core.

Cr-Ni-Mo steels are currently used for parts requiring high resilience, toughness and fatigue crack growth resistance, as well as resistance to wear and fatigue crack initiation due to the high surface hardness imparted by surface heat treatments such as cementing, nitriding and carbonitriding[1,2,9]. A nickel content of 1.5 to 4.5% wt increases the yield strength, resilience and fracture toughness (which invariably includes fatigue crack growth and impact resistances) of structural steels. Chromium enhances the wear resistance of steels due to the formation of chromium carbide, while molybdenum protects against the weakening of tempering and promotes the uniformity of steels processed for large thicknesses[9].

Figure 1 shows a schematic of the intermediate gear set evaluated in this case study.

2.1. *Description of the failure*

Figure 2 shows a pinion tooth subjected to failure analysis due to the extensive deterioration it suffered during in-service conditions. The types of damage typically found in the contact line of assessed teeth were classified as scaling and pitting, which undoubtedly resulted from fragmentation of the case hardened layer.

However, the progressive enlargement of scales and pits can lead to a type of damage known as cyclone, which is illustrated in Figure 2.

2.2. *Procedures*

To discover the root causes of the intermediate pinion shaft failure, the following experimental procedures were carried out in chronological sequence.

- Chemical analysis of the base material by spark source optical emission spectrometry at ambient temperature and 43% relative humidity (average of two samples).
- Full documentation of the characteristics of the pinion tooth damage through digital images recorded in macro-mode.
- Visual inspection of damage using a binocular stereomicroscope.
- Tensile tests of round cross section specimens according to the DIN 50125 standard[14] in ambient conditions (average of three specimens).
- Charpy impact tests of type-A test coupons in ambient

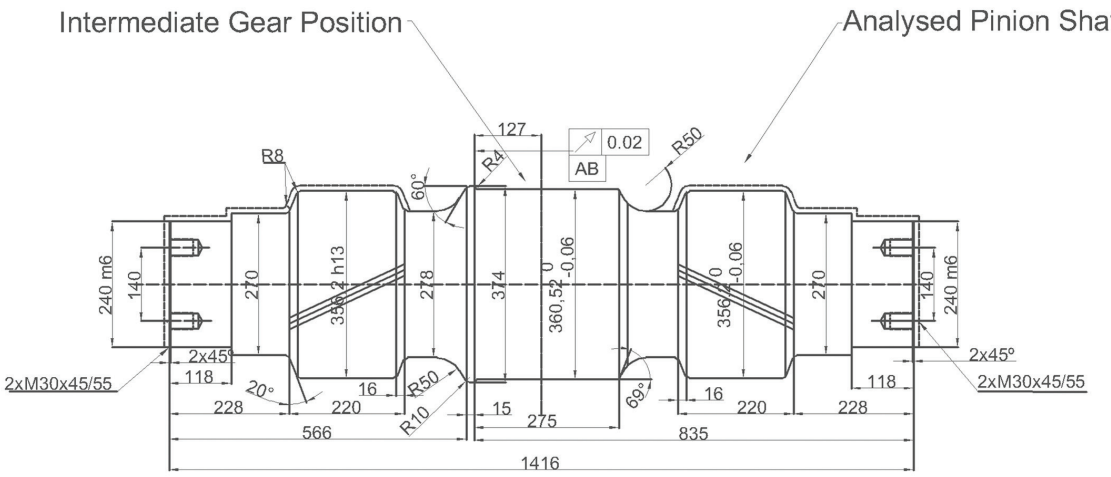

Figure 1. Draft of the intermediate reducer shaft, where the fractured pinion shaft is indicated by an arrow. The location of the corresponding idler (intermediate) gear is also arrowed.

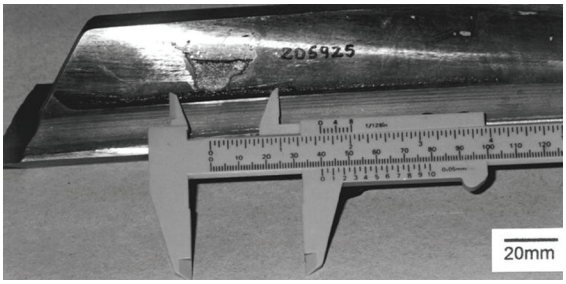

Figure 2. Representative case of a badly damaged pinion tooth surface.

conditions, according to the DIN EN10045 standard[15] (average of three specimens).

- Rockwell macrohardness measurements (HRC - 150 kgf) of the tooth core, according to the ASTM E-18 standard[16].
- Vickers microhardness profiles (HV - 200 gf) along the case-hardened layer of pinion teeth, according to ASTM E-384[17], adjacent to and far from cyclone-type damage (see Figure 2).
- Microstructural analysis of cross-section metallographic planes in the vicinity of substantial mechanical damage in the pinion tooth, with and without chemical etching.
- High magnification density contrast imaging of the cemented, hardened and tempered microstructure by Scanning Electron Microscopy (SEM) in backscattered electron mode, along with Energy Dispersive X-Ray (EDS) microchemical analysis.

3. Results and Discussion

3.1. *Chemical analysis*

Table 1 describes the average chemical composition (wt %) of the pinion core material, which is totally consistent with the SAE 8620 specification[12]

Table 1. Chemical composition (wt %) of the pinion tooth base material investigated here. Average of two evaluated samples.

Chemical element	Weight %	SAE 8620 specification
C	0.20	0.15-0.20
Si	0.23	≤ 0.40
Mn	0.60	0.40-0.60
P	0.012	0.035 (Max.)
S	0.016	0.035 (Max.)
Cr	1.54	1.50-1.80
Ni	1.46	1.40-1.70
Mo	0.28	0.25-0.35

3.2. *Macroscopic inspection*

Figure 3 depicts the contact line of the counterpart gear tooth, clearly showing the presence of pits. This is normally the first stage of RSCF under relatively low applied stresses, and is corroborated here by the absence of noticeable plastic deformation of the inspected surface. In fact, in this position (contact or pitch line) the maximum bearing (compression) stresses develop between the pinion and its counterpart gear surfaces. On the other hand, the peak location of subsurface stress resulting from the sum of rolling and sliding stresses occurs elsewhere below the surface.

Figures 4a and 4b show the so-called cyclone pattern shown in Figure 2, developed under surface contact fatigue in the pinion pitch line, which is created by continuous and extensive fragmentation of the case hardened layer of the pinion tooth in the rolling direction.

3.3. *Tensile and impact tests*

Table 2 describes the tensile properties of yield stress (σ_{ys}), ultimate tensile strength (σ_{uts}), elongation (E_F) and reduction of area (A_F) at fracture, as well as the Charpy impact absorbed energy (CIAE) of the pinion tooth core material.

The results listed in Table 2 qualify the SAE 8620 type steel employed for the application in question. Indeed, as mentioned earlier, damage was detected only on the cemented and subsequently heat-treated hard surface layer of the pinion shaft.

3.4. *Macro- and microhardness*

Rockwell macrohardness measurements of the pinion tooth core indicated values ranging from 34.0 to 42.7 HRC, which are very close to the 35.0-43.0 HRC specified in the design stage.

Microhardness values are plotted in Figure 5, where the data points indicate a hardened case depth of 3.2 to 3.5 mm, assuming that the nominal thickness of the cemented layer corresponds to the position where a value of 550 $HV_{0.2}$ is reached from the top layer surface after the Q&T heat treatment, according to the DIN 50190 standard. Compared to the typical target value of 2.6 mm specified for this pinion shaft size, it can be concluded that the thickness of the hardened case exceeded 0.6-1.1 mm.

Figure 3. Detailed view of the contact line and neighboring regions of counterpart bigger gear viewed with a binocular stereoscope (microscopic pitting).

This is a significant point in this case study, because the pertinent literature often mentions that to avoid the coincidence between maximum localized subsurface Hertzian (shear) stress and the critical transition region between the cemented layer and pinion core, designers often resort to over thick carburized layers.

As it will be seen later, this stratagem appears to be effective in avoiding subsurface crack initiation due to contact fatigue, although it will inevitably go hand in hand with some drawbacks such as cemented layers with very brittle microstructures.

According to the plotted $HV_{0.2}$ microhardness data in Figure 5, no evidence of surface decarburization of the cemented pinion during consecutive Q&T heat treatment can be detected.

3.5. *Optical analysis of the microstructure*

Figure 6 shows the typical microstructure of a pinion tooth core after Q&T heat treatment, which appears to be homogeneous and to consist mainly of tempered martensite, a highly desirable microconstituent for the mechanical application of the alloy steel in question.

Figure 7 displays various pit morphologies developed on the pitch line surface of a case hardened pinion tooth. Note that fatigue cracks grow and branch out from the pit tips, although cracking remains restricted to the cemented layer due two main factors: (i) cracks face a much tougher microstructure in the pinion core, and (ii) driving force for crack growth due to the sum of rolling and sliding (shear) stresses decays rapidly towards the tooth core from the peak value attained elsewhere below the rotating component surface. This is especially true when a thicker than normal cemented layer is identified and measured, according to plotted data points in Figure 5. It can be assumed that the state of deterioration of the pinion surface when the Figure 7 image was captured is compatible with the degradation stage documented in Figure 3 for the tooth belonging to

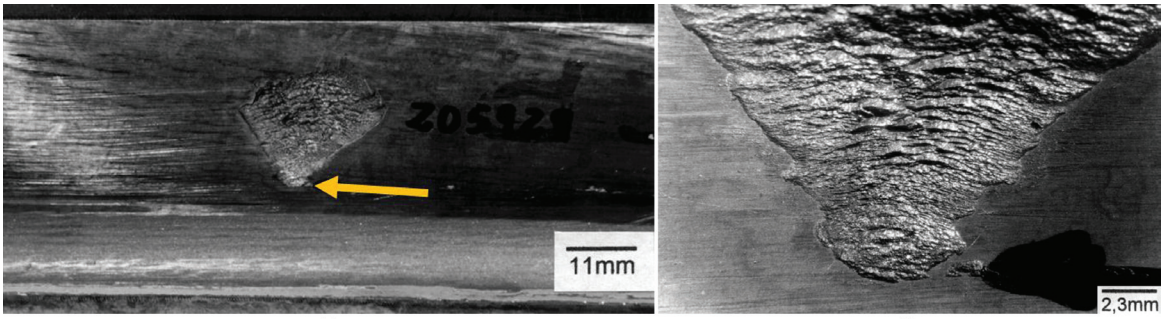

Figure 4. Surface contact fatigue damage of the cemented and subsequently Q&T SAE 8620 steel pinion tooth flank: (a) Typical cyclone morphology, with the likely initiation site indicated by an arrow; (b) Detailed view of the formed cavity (classified as severe spalling) seen under a binocular stereoscope.

Table 2. Quasi-static monotonic tensile and Charpy impact properties of the pinion core material. Average of three test specimens for each type of mechanical test, and corresponding standard-deviations.

Material/Property	σ_{ys} (MPa)	σ_{uts} (MPa)	E_F (%)	A_F (%)	CIAE (J)
Pinion tooth	693.1 ± 31.8	983.3 ± 39.9	20.4 ± 0.9	58.5 ± 2.4	35.2 ± 1.5

the counterpart bulkier gear (keeping in mind that the view planes of Figures 3 and 7 are orthogonal each other).

Figure 8 shows several subsurface cracks emerging from the pinion tooth surface, causing the release of fragments of the hardened case thus favoring the generation of cyclone type damage, as already depicted in both the Figures 2 and 4.

Furthermore, it can be inferred that the fragments detached from the wear surface are the net result of compressive loads, which give rise to combined rolling and sliding loading modes between the parts in contact with each other. This induces an ever-increasing wear rate of their materials, which in turn impairs the performance of entire mechanical system[5-8]. It is worth noting that the pinion (smaller gear) invariably degrades at a faster rate than the corresponding gear (larger gear) because it naturally rotates at higher angular velocities (rotations per unit time) than the latter component.

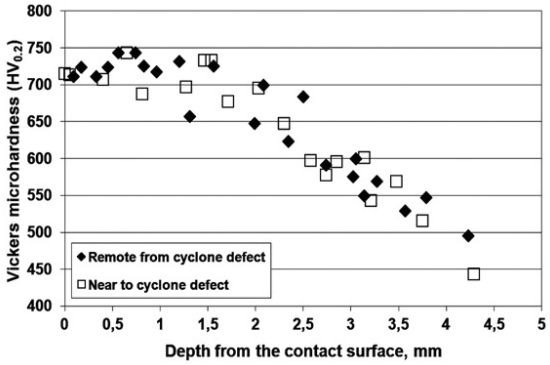

Figure 5. $HV_{0.2}$ microhardness profiles of the case hardened layer in the wake of two distinct linear paths of a pinion shaft tooth flank containing a cyclone type defect.

Since the above described analysis was unable to provide information to fully identify the root causes of the failure, indicating only the mechanisms whereby pits, scales, cracks and the cyclone-like damage were generated, a thorough micrographic inspection was conducted along the edge of the pinion tooth. However, at this time no surface chemical etching was employed to observe the sample.

The micrograph in Figure 9 shows the examined tooth root where grain boundaries are quite visible due the presence of brittle films of metal oxides and/or Fe_3C. These constituents are potential sites for crack nucleation and offer preferential pathways for crack propagation.

Cracks tend to form a common plan of progression, naturally following the path of least resistance, such as the intergranular fracture weakened by the presence of carbides and/or oxides at grain boundaries. As mentioned earlier,

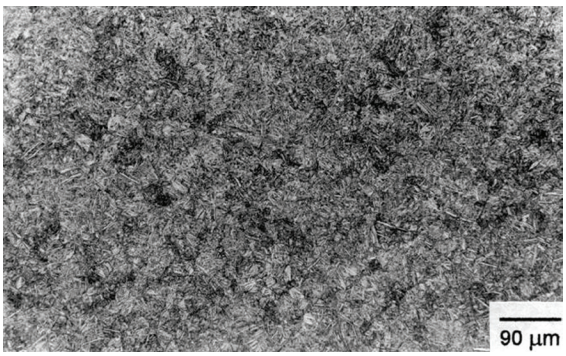

Figure 6. Typical microstructure of the pinion tooth core. Etched with Nital 2%.

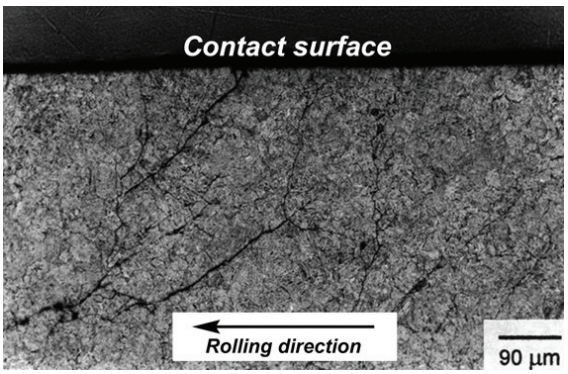

Figure 8. Emerging cracks in a slightly worn portion of the contact surface in the case hardened pinion tooth. Etched with Nital 2%.

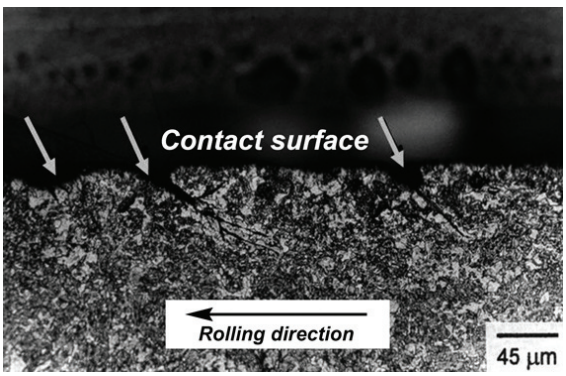

Figure 7. Cross-section view of a pinion tooth showing several pits (indicated by arrows) from which fatigue cracks branch out towards the bulk microstructure during periodic contact with the counterpart gear tooth surface. Etched with Nital 2%.

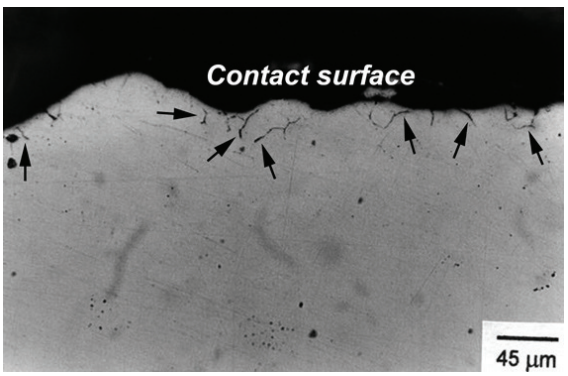

Figure 9. Evidence of secondary phase(s) in prior austenite grain boundaries (i.e., martensite packet bounds) at the root region of a cemented pinion tooth, without chemical etching. An identical pattern was sometimes observed at the flank of other pinion teeth.

grains or grain agglomerates are pulled out from the surface, generating pits and wear debris. Once pits have been formed, the pitting mechanism follows a geometric discontinuity that concentrates stresses, at which point nucleation and subsequent crack propagation phenomena are absolutely viable and occur readily, leading to increasingly expanding and geometrically complex damage. Furthermore, it is very important to emphasize the deleterious effect of oxides and carbides already in the stage of crack nucleation, since they are known to be brittle phases that can induce severe stress concentration.

Figure 10 shows the role of the microstructure of the cemented steel layer, in terms of how the nature, content and spatial distribution of inclusions affect the removal rate of material from the pitch line in the pinion tooth. The left hand arrow shows a hard particle in the cemented layer, thus elucidating its role as stress concentrator favoring matrix cracking. The right hand arrow points out the detachment of a relatively massive case hardened fragment, hence leading to pitting (mass loss) and raising surface roughness of the rotating component.

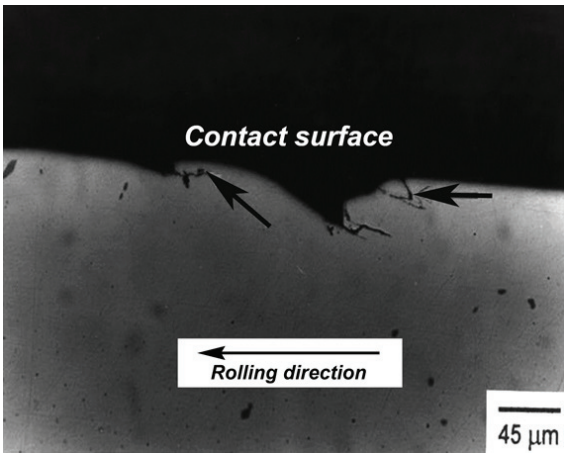

Figure 10. Brittle particles at the surface of the cemented layer (indicated by arrows), which are about to be dislodged, resulting in pits and contact surface unevenness. No etching.

3.6. *Scanning Electron Microscope (SEM) analysis*

To complete the identification of microconstituents at grain boundaries in the tempered martensitic microstructure at the flanks of the failed pinion tooth, a SEM analysis in backscattered electron (BSE) mode was first performed of this particular region. Figure 11a confirms the presence of a secondary phase in-between neighboring martensitic packets (i.e., prior austenitic grains). SEM-BSE allows phases differentiation on the basis of their distinct densities, where lighter colors refer to higher densities and vice-versa.

As can be seen, the density of the vermicular phase located inside the packet or grain boundary network is much lower than that of the metallic matrix (SAE 8620 steel), thus reinforcing the hypothesis of a massive presence of cementite in that region. Figure 11b proves the existence of a continuous brittle film along the boundaries of the martensite (prior austenite) on the surface of the pinion's cemented layer. Energy dispersive X-ray microchemical analysis of intergranular and intermetalic phases seen in Figure 11 attested them as Fe_3C and CrNiMo microconstituents, respectively.

4. Conclusions

A visual inspection of the damage suffered by the case hardened pinion tooth made of SAE 8620 type steel showed that the failures originated from surface contact fatigue, more specifically through pitting mechanism.

Chemical composition, as well as mechanical properties of the pinion core met all the design specifications, and

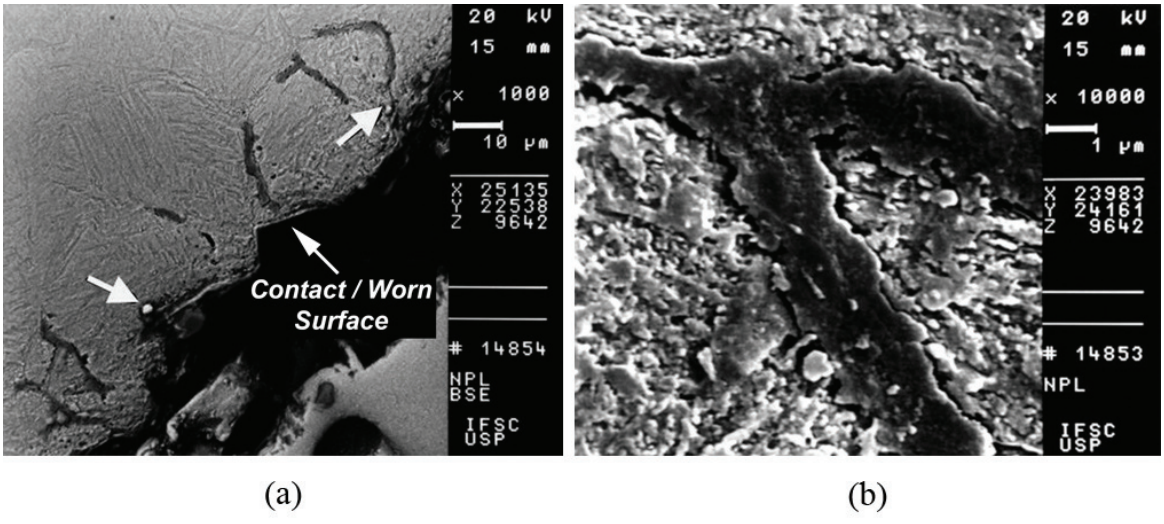

Figure 11. (a) Vermicular morphology of cementite phase at grain boundaries. The intermetallic particles indicated by arrows are much denser than those of an average steel matrix; (b) Detailed view of the continuous cementite film located at the grain boundaries. Etched with Nital 2%.

microhardness measurements indicated that, based on the attained values of surface contact stresses, the goals of pinion cementation were met.

However, the cemented layer in question was found to be thicker than that specified during the pinion design, indicating excess concentration of carbon in the available contacting surface of the pinion tooth. Optical and electronic scanning microscopies allied with the microhardness measurement of the cemented layer microstructure revealed an enhanced cracking process in the pitch line and the massive presence of a secondary filiform phase in the prior austenite grain boundaries (i.e., martensite packet bounds) at the root and top regions of the pinion tooth. EDX microprobe analysis identified the intergranular phase as basically composed by Fe_3C, a powerful microstructural stress concentrator when present in this form, causing embrittlement of the grain boundaries. Therefore, an over thick cemented layer in conjunction with threadlike intergranular Fe_3C facilitated surface crack nucleation and propagation due to repeated compressive contact loads (i.e., RSCF mechanism), giving rise to pit formation in the wear area of the pinion teeth.

The progression of this mechanism in the contact line between the case hardened pinion and its larger counterpart gear caused the former component to fail by cyclone-like damage.

The surface contact fatigue process was therefore the failure mechanism of the part, notwithstanding the root cause of pinion failure was its misguided cementation process. Accordingly, a more detailed study should be conducted to improve the efficiency of this secondary manufacturing practice in terms of batch time, temperature and carbon content, to avoid problems in similar structural metallic components.

Acknowledgements

To the Federal University of São Carlos – Sorocaba City Campus, Sorocaba-SP, CEP 18052-780, Brazil.

References

1. Norton RL. *Projeto de Máquinas: uma Abordagem Integrada.* 2. ed. Porto Alegre: Bookman; 2004.
2. Niemann G. *Elementos de Máquinas*. 3. ed. São Paulo: Edgar Blücher; 1995.
3. Das CR, Albert SK, Bhaduri AK, Ray SK. Failure Analysis of a Pinion. *Engineering Failure Analysis*. 2005; 12:287-298. http://dx.doi.org/10.1016/j.engfailanal.2004.03.010
4. Suresh S. *Fatigue of Materials*. 2nd ed. Cambridge: Cambridge University Press; 1998. http://dx.doi.org/10.1017/CBO9780511806575
5. Suh NP. The Delamination Theory of Wear. *Wear.* 1973; 25:111-124. http://dx.doi.org/10.1016/0043-1648(73)90125-7
6. Bayrakceken H. Failure Analysis of an Automobile Differential Pinion Shaft. *Engineering Failure Analysis*. 2006; 13:1422-1428. http://dx.doi.org/10.1016/j.engfailanal.2005.07.019
7. Fernandes PJL. Tooth Bending Fatigue Failures in Gears. *Engineering Failure Analysis*. 1996; 3:219-225. http://dx.doi.org/10.1016/1350-6307(96)00008-8
8. Fernandes PJL, McDulling C. Surface Contact Fatigue in Gears. *Engineering Failure Analysis*. 1997; 4:99-107. http://dx.doi.org/10.1016/S1350-6307(97)00006-X
9. Basan R, Franulovic M, Lengauer W, Krizan B. Rolling-Sliding-Contact Fatigue Damage of the Gear Tooth Flanks. *Engineering Review.* 2010; 30:37-46.
10. Hyde RS. *Contact Fatigue of Hardened Steel*. ASM International; 1996. ASM Handbook. v. 19, Fatigue and Fracture.
11. Peterson R, Rice SL. *Case Crushing of Carburized and Hardened Gears.* SAE Technical Paper 610034; 1961.
12. Society of Automotive Engineers. *SAE-AMS 6274:* Specification for steel, bars, forgings, and tubing, 0.50Cr - 0.55Ni - 0.20Mo (0.18 - 0.23C). Aerospace Material Standards. American Society for Testing and Materials; 2011.
13. Deutsches Institut für Normung. *DIN 50190*: Standard for hardness depth of heat-treated parts; determination of the effective depth of hardening after flame or induction hardening. DIN; 1979.
14. Deutsches Institut für Normung. *DIN 50125*: Standard testing of metallic materials - tensile test pieces. DIN; 2009.
15. Deutsches Institut für Normung. *DIN EN 10045*: Standard Charpy impact test on metallic materials: test method. DIN; 1994.
16. American Society for Testing and Materials. *ASTM E-18:* Standard test methods for Rockwell hardness of metallic materials. ASTM; 2014.
17. American Society for Testing and Materials. *ASTM E-384:* Standard test method for Knoop and Vickers hardness of materials. ASTM; 2011.